INTERNATIONAL JOURNAL FOR NUMERICAL METHODS IN FLUIDS, VOL. 5, 545–560 (1985)

FINITE ELEMENT ANALYSIS OF INCOMPRESSIBLE LAMINAR BOUNDARY LAYER FLOWS*

SANG-WOOK KIM†

School of Aeronautics and Astronautics, Purdue University, West Lafayette, Indiana 47907, U.S.A.

AND

F. R. PAYNE‡

Aerospace Engineering Department, University of Texas at Arlington, Arlington, Texas 76019, U.S.A.

SUMMARY

A numerical procedure was developed to solve the two-dimensional and axisymmetric incompressible laminar boundary layer equations using the semi-discrete Galerkin finite element method. Linear Lagrangian, quadratic Lagrangian, and cubic Hermite interpolating polynomials were used for the finite element discretization; the first-order, the second-order backward difference approximation, and the Crank–Nicolson method were used for the system of non-linear ordinary differential equations; the Picard iteration and the Newton–Raphson technique were used to solve the resulting non-linear algebraic system of equations. Conservation of mass is treated as a constraint condition in the procedure; hence, it is integrated numerically along the solution line while marching along the time-like co-ordinate. Among the numerical schemes tested, the Picard iteration technique used with the quadratic Lagrangian polynomials and the second-order backward difference approximation case turned out to be the most efficient to achieve the same accuracy. The advantages of the method developed lie in its coarse grid accuracy, global computational efficiency, and wide applicability to most situations that may arise in incompressible laminar boundary layer flows.

KEY WORDS Boundary Layer Flows Time-like Co-ordinate Space-like Domain Inviscid Tangential Velocity Pressure Gradient

INTRODUCTION

Owing to the importance of boundary layer flow problems in engineering applications, researchers in the area are quite active at present as well as in the recent past.

The most salient and historically the first similarity solution of the boundary layer equations is the Blasius flat plate solution[1] which appeared in 1908. Rather more general similarity solutions are those of Falkner and Skan,[1] Hartree[1] and others.[2] In these methods the fluid viscosity must be constant and the outer inviscid flow field takes certain specific forms such as a power law, so that similarity is achieved. These requirements are relaxed in the yet more general formulations such as the Mangler–Levy–Lee transformation method[3] or the Blasius series expansion method[2] which can model non-similar flows. The resulting transformed boundary layer equations are usually solved by a finite difference method or by a finite element method. Examples in these areas are found in the works of Bismarck-Nasr[3] and Smith and Clutter.[4] Even in these non-similar

*This work was done when the first author was at the University of Texas at Arlington as a visiting assistant professor.
†Post-Doctoral Research Associate
‡Professor

0271–2091/85/060545–16$01.60

Received 10 August 1983
Revised 5 March 1984 and 7 January 1985

solution techniques, the fluid viscosity cannot vary freely across the boundary layer in order for the solution technique to be applicable. These techniques yield quite accurate results for laminar boundary layer flows but cannot be extended to turbulent flows owing to the constraints laid upon the physical properties, i.e. the apparent viscosity is a strong function of the normal co-ordinate and, to a lesser extent, of the tangential co-ordinate in turbulent flows.

A classical solution scheme distinct from the similarity methods and usually termed the momentum integral method assumes a form for the velocity profile inside the boundary layer; substitution of this profile into the integral form of the momentum equation results in an ordinary differential equation which can be solved easily. Pohlhausen's,[1] Thwaites',[5] and Head's[5] methods belong to the class of momentum integral methods. A review of the existing boundary layer solution techniques reveals that the momentum integral type formulations are generally inaccurate compared to other laminar boundary layer solution techniques. Therefore, applications of the integral type methods to laminar boundary layer flows are quite limited. Nevertheless, the momentum integral type formulations are an important technique for turbulent boundary layer flows: this is due to its capability to incorporate simple turbulence models.

Owing to the lack of generality and inadequacy of the methods described, emphasis has been upon developing solution techniques which are both accurate and extendable to turbulent boundary layer flows. Among these are those of Gibson and Rodi,[6] Lynn and Alani,[7] Baker[8] and Soliman and Baker.[9,10] Lynn and Alani used a least squares finite element method to solve a class of incompressible laminar boundary layer flows. Gibson and Rodi used a finite difference method to solve a highly curved incompressible turbulent shear layer. Baker solved incompressible laminar and turbulent boundary layer flows over a flat plate by the semi-discrete Galerkin finite element method which is similar to the method developed in the present study. Soliman and Baker[9,10] extended application of the method used by Baker[8] to turbulent boundary layer flows with pressure gradients and also presented some results on convergence study. All these methods solve the boundary layer equations using primitive variables, i.e. the unknowns are velocity components. One of the advantages of using primitive variables lies in its versatility to accommodate discontinuous boundary conditions such as those arising in boundary layer control problems via suction or injection. It is believed that these three solution techniques and the present study can be extended to compressible turbulent boundary layer flows. In general, it is not appropriate to say which finite element method is more accurate since we can obtain as accurate a numerical solution as we wish, if the method is convergent, by refining the meshes until the round-off errors become dominant. Therefore, efficiency and versatility are of paramount importance when comparing different finite element methods. The present method has been tested against a number of incompressible laminar boundary layer flows. They are;[11,12] flow over a flat plate, the retarded Howarth flow, flow over a wedge, plane stagnation flow, axisymmetric stagnation flow, flow over a circular cylinder, flow in the wake of a flat plate, a uniform suction flow on a flat plate, flow over a cone and flow over a sphere. Computational results compared favourably with results obtained by other investigators. A few of the computational results are presented herein.

BOUNDARY LAYER EQUATIONS

The incompressible laminar boundary layer equations are given as[1]

$$uu_{,x} + vu_{,y} = UeUe_{,x} + \frac{1}{\rho}\tau_{yx,y}, \tag{1}$$

$$(r_0^m u)_{,x} + (r_0^m v)_{,y} = 0, \tag{2}$$

where (1) is a momentum equation, (2) is a conservation of mass equation, the co-ordinate system (x, y) is defined locally such that the time-like co-ordinate x is tangential to the surface and y is normal to the surface of the submerged body, u and v are velocity vectors in the x and y directions, respectively, ρ is the density of the fluid, $Ue(x)$ is the x-component velocity as y approaches infinity, r_0 is a radius of a body of revolution, $m = 0$ for the two-dimensional flow case, $m = 1$ for an axisymmetric flow case, and $(\ )_{,a}$ represents differentiation of $(\ )$ with respect to a. The shear stress for the incompressible laminar case is given as

$$\tau_{yx} = \mu u_{,y}, \tag{3}$$

where μ is the molecular viscosity of air. The boundary conditions for both flow cases are given as

$$u(x, y) = 0, \quad \text{at } y = 0, \tag{4}$$

$$v(x, y) = v_1, \quad \text{at } y = 0, \tag{5}$$

$$u_{,y}(x, y) = 0, \quad \text{as } y \to \infty. \tag{6}$$

A characteristic of boundary layer flows is the extremely small viscous layer thickness which is order of $1/\sqrt{R}$, where R is the Reynolds number defined as $U_\infty L/v$ and $u/Ue = 0{\cdot}99$ is customarily used to define the boundary layer thickness, L is the characteristic length in flow direction, and U_∞ is the reference velocity. For computational convenience, we introduce a set of co-ordinate transformations and non-dimensionalization parameters. Setting $\hat{x} = x/L$, $\hat{y} = y\sqrt{R}/L$, $\hat{u} = u/U_\infty \hat{v} = v\sqrt{R}/U_\infty \hat{U}e = Ue/U_\infty$ and $\hat{r}_0 = r_0/L$ in equations (1)–(6), and deleting the superscript $(\hat{\ })$ for notational convenience yields

$$uu_{,x} + vu_{,y} = UeUe_{,x} + (u_{,y})_{,y}, \tag{7}$$

$$(r_0^m u)_{,x} + (r_0^m u)_{,y} = 0. \tag{8}$$

Note that the forms of the boundary layer equations are independent of the Reynolds number. It is found that $u_{,y} = 0$ is equivalent to $u \to Ue$ as y approaches infinity. We used $u_{,y} = 0$ in our finite element analysis and found that the pressure gradient term, $UeUe_{,x}$ developed the external inviscid velocity in close agreement with the prescribed external inviscid velocity distribution along the flow direction. Since the boundary layer equations are defined on an infinite domain, it is necessary to set up a finite domain for our numerical analysis. The computational domain in the direction normal to the surface is taken to be several boundary layer thickness apart from the surface of the submerged body.

FINITE ELEMENT EQUATIONS

The boundary layer equations are parabolic, partial differential equations in the direction tangential to the surface. Based on the similar parabolic nature of the boundary layer equations to the standard parabolic, partial differential equations arising in the mathematical description of a class of time-dependent physical problems, such as heat conduction problems, we propose to solve the boundary layer equations by the semi-discrete finite element method in which the direction normal to the surface is discretized by a number of finite elements and the time-like direction remains continuous. Therefore, the proposed scheme takes the form of initial-boundary value solution techniques. The required initial conditions are different depending upon the interpolation polynomials used as well as the difference approximations employed. Owing to the way the initial conditions are used in the iterative solution procedure, they are discussed in a separate section.

The standard semi-discrete Galerkin finite element method can be found in References 13, 14 or 15. We simply state the results here. The semi-discrete finite element equation for the momentum part of the boundary layer equations for both of the two-dimensional and the axisymmetric cases is obtained as[11]

$$A_{ij}\dot{u}_j + B_{ij}u_j + K_{ij}u_j - F_i = 0, \tag{9}$$

where

$$A_{ij} = \int_0^l (u_k\phi_k)\phi_i\phi_j \,\mathrm{d}y,$$

$$B_{ij} = \int_0^l (v_k\phi_k)\phi_i\phi_{j,y} \,\mathrm{d}y,$$

$$K_{ij} = \int_0^l \phi_{i,y}\phi_{j,y} \,\mathrm{d}y,$$

$$F_i = \int_0^l UeUe_{,x}\phi_i \,\mathrm{d}y$$

and the superscript ($\dot{}$) denotes the derivative of u in the time-like direction; the u_js denote nodal degrees of freedom for u for the Lagrangian interpolation case, and u and $u_{,y}$ for the Hermite interpolation case; the v_js denote nodal degrees of freedom for v; the ϕs are the global basis polynomials; and $\{y | y \in (0, l)\}$ denotes the space-like domain. In equation (9) the global finite element equations were derived using the global interpolating polynomials for convenience in developing the theory. But in computer implementation, the finite element matrices are derived for each element and then assembled to obtain the global equations. The conservation of mass equation is treated as a constraint condition and integrated numerically along the solution line as we proceed in the tangential direction. The nodal values of the normal velocity component become

$$v(x, y_j) = \left\{ \int_{y_{j-1}}^{y_j} \dot{A}_k\phi_k \,\mathrm{d}y - r_0^m(x)v(x, y_j) \right\} / r_0^m(x), \tag{10}$$

where $\dot{A}_k$ denotes $(r_0^m u)_{,x}$ at nodal points. The integration in equation (10) was evaluated using the Gauss quadrature rule.[13]

FINITE DIFFERENCE APPROXIMATIONS

The system of first-order non-linear ordinary differential equations, (9), derived through the semi-discrete Galerkin finite element formulation, is also defined on the same locally orthogonal curvilinear co-ordinates on which the boundary layer equations are defined. There exist several systems of ordinary differential equation integrators; multi-step forward difference methods, multi-step backward difference methods, the Crank–Nicolson method, the Runge–Kutta method, and modified versions of these methods. These are discussed in detail by Zlatev and Thomson[16] with regard to accuracy, efficiency and stability. In the computational experiments, they tested these systems of ordinary differential equation integrators by applying them to a system of ordinary differential equations derived through a semi-discrete Galerkin finite element formulation of a linear transient heat conduction equation. They showed that the Crank–Nicolson method is not attractive, owing to the enormous error encountered especially when the matrices are stiff and the step sizes are large. They also showed that the multi-step backward

difference method was the best system of ordinary differential equation integrators, for the problem considered, owing to its efficiency, accuracy and irrelevance to the stability requirement.[16]

In boundary layer calculations, one needs to use an extremely fine mesh near the separation region to better estimate the separation point, whereas, in the accelerating region, a coarse mesh can be used for computational efficiency. Therefore, any method which requires an extremely fine mesh to achieve convergence does not seem appropriate for boundary layer calculations. Also, the propagation nature of the momentum equation in the time-like direction is not as simple as in the transient heat convection-diffusion equation, since the derivative of the tangential velocity in the time-like direction is coupled with the tangential velocity itself.

We choose to test the multi-step backward difference approximation method and the Crank–Nicolson method in the present study. The one-step difference approximation and the two-step difference approximation are considered for the multi-step backward difference case. As shown in the following discussions, any higher order difference approximation in the flow direction can be easily incorporated into the formulation.

For the one-step difference approximation, we can write the derivative of the nodal degree of freedom, u_j, in the time-like direction as

$$\dot{u}_j = \frac{u_j^n - u_j^{n-1}}{\Delta x}, \tag{11}$$

where the superscripts n and $n-1$ represent the present and the one-step previous line-levels, respectively, and Δx is the mesh size in the one-step difference approximation. Equation (11) applies for both of the Lagrangian and the Hermitian interpolation cases. Substituting equation (11) into equation (9) yields:

$$\left[\frac{1}{\Delta x}A_{ij} + B_{ij} + K_{ij}\right]u_j^n = \frac{1}{\Delta x}A_{ij}u_j^{n-1} + F_i. \tag{12}$$

For the two-step approximation, we can write

$$\dot{u}_j = \frac{3u_j^n - 4u_j^{n-1} + u_j^{n-2}}{2\Delta x}, \tag{13}$$

where the notations used are the same as in equation (11). Substituting equation (13) into equation (9) yields

$$\left(\frac{3}{2\Delta x}A_{ij} + B_{ij} + K_{ij}\right)u_j^n = \frac{4}{2\Delta x}A_{ij}u_j^{n-1} - \frac{1}{2\Delta x}A_{ij}u_j^{n-2} + F_i, \tag{14}$$

where the notations used are the same as in equation (11).

For the Crank–Nicolson method,[16] we use the approximations that

$$u_j = \tfrac{1}{2}(u_j^n + u_j^{n-1}), \tag{15}$$

$$v_j = \tfrac{1}{2}(v_j^n + v_j^{n-1}), \tag{16}$$

$$\dot{u}_j = \frac{1}{\Delta x}(u_j^n - u_j^{n-1}). \tag{17}$$

Substituting equations (15) and (17) into equation (9) yields

$$\left(\frac{1}{\Delta x}A_{ij} + \tfrac{1}{2}B_{ij} + \tfrac{1}{2}K_{ij}\right)u_j^n = \left(\frac{1}{\Delta x}A_{ij} - \tfrac{1}{2}B_{ij} - \tfrac{1}{2}K_{ij}\right)u_j^{n-1} + \tfrac{1}{2}(f^n + f^{n-1}), \tag{18}$$

where A_{ij} and B_{ij}, given in equation (9), are evaluated using equations (15) and (16), respectively, and the notations used are the same as in equation (11). Incorporating initial condition data and the boundary conditions into equations (12), (14) or (18) completes the system of non-linear algebraic equations to be solved for the nodal unknowns.

INITIAL CONDITION DATA AND INITIAL GUESS

One needs to provide the initial condition data to be used in equations (12), (14) or (18). For the Lagrangian interpolation case, the tangential velocity data are required: and for the Hermitian interpolation case, both the tangential velocity data and the normal direction derivative of the tangential velocity data are required as initial condition data. In the numerical procedure developed herein, the conservation of mass equation is treated as a constraint condition. Therefore, initial condition data for the normal velocity component are not required to start the iteration, which is an advantage of the present method.

For the one-step difference approximation and the Crank–Nicolson cases, initial condition data are needed on the starting line; and, for the two-step difference approximation case, the initial condition data are required on two starting lines. If the initial condition data were prepared from an experiment, then the one-step difference approximation method can be used to prepare the data on the second line. But the optional approach requires an assurance that the one-step difference approximation method yields an accurate and convergent solution. The convergence natures of both difference approximation methods are proved through computational experiments.

Picard and Newton–Raphson[13] iteration techniques were used to solve the algebraic equations (12), (14) or (18).

For the present boundary layer study, we use the solutions on the previous line-level (equivalent to time-level for transient problems) as the initial guess for the working line-level.

To facilitate initial condition data preparation, the initial condition data for the normal velocity are set equal to zero, which amounts to setting B_{ij} equal to zero in equations (12), (14) or (18) at the starting of the iterative solution procedure. In this approach, the number of iterations is increased only by 1 or 2 at the very beginning of the computation. As soon as we pass through the first solution line, then the usual initial guess procedure is resumed. Therefore the total number of iterations throughout the whole solution procedure is not significantly affected.

REGRID

In most boundary layer flows, the boundary layer thickness grows along the flow direction. Therefore, it is necessary to expand the computational domain in the normal to the surface direction to take into account the growing boundary layer thickness. The domain in the normal to the surface direction was expanded about 35 per cent whenever $u(x, l)/Ue(x)$ became less than a prescribed value at the outer edge of the computational domain, where $Ue(x)$ is the flow direction inviscid velocity. $u(x, l)/Ue(x)$ equal to 0·99988 (or 0·999) was used in the present study. The tangential velocity data on the expanded portion of the domain was set equal to $Ue(x)$, but the normal velocity data are not required for the reasons discussed previously.

A regrid scheme was used to discretize the resulting expanded domain, in which the total number of nodes and the total number of elements remain constant. The nodal velocity components and their derivatives inside the unexpanded domain were obtained by interpolating the solutions on the line. Another possibility of expanding the domain in the normal direction is to add more elements and nodes for the expanded portion of the domain as has been used by Lynn and

Alani.[7] On the other hand, Soliman and Baker[9,10] assumed that the boundary layer thickness is a function of tangential co-ordinate and incorporated it into the finite element equation itself. For real application problems, e.g. boundary layer flow over an aerofoil, boundary layer thickness grows steadily under favourable pressure gradient and rapidly under adverse pressure gradient, and it is usually unknown until the problem is solved. For versatility in application and for computational efficiency, the regrid scheme was used in the present work.

CONVERGENCE STUDY

The theory of convergence and accuracy of the finite element method is well established for linear elliptic or linear parabolic partial differential equations. However, it has not yet been fully studied for other types of partial differential equations, especially for non-linear partial differential equations.

In linear parabolic, partial differential equations, the error estimate can be performed separately for the semi-discretization part of the finite element formulation in the space domain and the difference approximation part in the time domain.[15] But the boundary layer equations are non-linear parabolic partial differential equations in the flow direction. In the present formulation, the discretization error in the time-like domain is fed back into the semi-discretization procedure of the space-like domain through the normal velocity calculation, equations (9) and (10). Also, the boundary layer equations are defined on an infinite domain. Hence, the extent of domain used in the numerical analysis will also affect the computational results. Therefore, the prior error estimate for linear parabolic partial differential equations cannot be applied directly to the present problem. Computational experiments on convergence behaviour are included in the example problems and discussed in the summary and conclusions.

CONVERGENCE CRITERIA

The non-linear algebraic system of equations was solved by the Picard and the Newton–Raphson iteration techniques until the convergence criteria were satisfied. There exist a number of convergence criteria one may choose to use. For the present work, we used the convergence criterion that

$$|1 - u_j^{n,p}/u_j^{n,p-1}| < \varepsilon, \tag{19}$$

where p denotes the iteration level for the solution vector u_js on the working line-level. A variable and its derivative have different order of convergence rates. Therefore, it would be reasonable to use different convergence criteria for the Hermite interpolation case and the Lagrangian interpolation case, if the same grid systems were used for both of the cases. There, $\varepsilon = 0{\cdot}000001$ was used as the convergence criterion for the Hermite interpolation case, and $\varepsilon = 0{\cdot}0000001$ for the Lagrangian interpolation case, unless otherwise specified.

COMPUTATIONAL EXPERIMENTS

The example problems presented herein are flow over a flat plate, a retarded Howarth flow, flow over a circular cylinder and flow over a cone. Since the major purpose was to investigate the uses and the advantages of the method developed, exhaustive study of each example flow was not attempted. Instead, the most important feature of any boundary layer study, i.e. evaluation of the wall shear stresses to estimate the overall skin friction of the submerged body, was exhaustively investigated using different meshes for each of the six schemes. A complete set of computa-

tional experiments can be found in Reference 11; only representative results are presented herein. The computational experiments presented herein were made on IBM 4341 machine at the University of Texas at Arlington.

Flow over a flat plate

The flat plate flow was used to study the convergence nature of the method and the effect of regrid on accuracy. Even though an exact solution does not exist, Blasius'[2] similarity solution can serve as an exact solution for the present study.

Consider a flat plate whose chord is 0·2 m submerged in a uniform flow of 40 m/s at an angle of attack of zero degrees. Throughout the computational experiments, the kinematic viscosity of air is taken to be $1{\cdot}46073 \times 10^{-5}$ m^2/s, the sea-level standard value. Setting the reference length to be 0·1 m yields the computational reference Reynolds number of $2{\cdot}396 \times 10^5$. Usually, transition from laminar to turbulent flow on a flat plate occurs near a Reynolds number of 5×10^5. Hence, this considers the largest usual Reynolds number for laminar flow over a flat plate. We calculate the boundary layer flow between $x = 0{\cdot}1$ m (mid-chord) and $x = 0{\cdot}2$ m (trailing edge) by the method developed. The initial velocity data were obtained from the Blasius' similarity solution.

Table I shows the required number of iterations and the computer time used, to satisfy the same convergence criteria of $\varepsilon = 0{\cdot}000001$, for the different numerical schemes. For all the cases in Table I, computation begins at $x = 0{\cdot}1$ m (or $\hat{x} = 1{\cdot}0$) It is found that the Newton–Raphson technique requires as many iterations and as much computer time as the Picard iteration technique for the Lagrangian interpolation case, and that the former technique is more efficient than the latter for the Hermite interpolation case. Nevertheless, the least amount of the computer time was required for the case of Lagrangian interpolation used with the Picard iteration technique. The coupling effect of the conservation of mass equation in the solution procedure seems to damage the quadratic convergence nature of the Newton–Raphson method.

In Reference 16 it was found that the Crank–Nicolson method was not so attractive, owing to enormous errors for a stiff system of ordinary differential equations. In the present work, the Crank–Nicolson method is found to be not attractive owing to the enormous number of iterations and the amount of computer time required. In the rest of the computational experiment, emphasis is laid on the Lagrangian interpolation with Picard iteration case; therefore the Crank–Nicolson method and the Newton–Raphson method are pursued no more.

For notational convenience, the superscript ($\hat{}$) is omitted in the following. The global convergence behaviour was studied using the mean square error norm of the tangential velocity component defined as

$$\|u\|_0 = \left\{ \int_\Omega (u_h - u_{\text{ref}})^2 \, dx \right\}^{1/2}, \tag{20}$$

where u_h represents the finite element solution, u_{ref} represents the Blasius solution and Ω represents the computational domain in the normal direction. The mean square error norms shown in Figures 1 and 2 are evaluated at $x = 1{\cdot}25$.

It is found in Figure 1 that the lower bound on convergence is determined by the grid size, Δx, and the order of difference approximation in the time-like co-ordinate as well as by the interpolation scheme in the space-like domain. For a linear parabolic problem, the lower bound will be determined by the discretization error in the time-like co-ordinate alone. Different lower bounds for different interpolation schemes in the space-like domain may have been caused by the feedback effect of the discretization error in the time-like co-ordinate into the semi-discretization procedure of the space-like domain through the normal velocity calculation. However, the differences

Table I. Convergence study

Iteration method	Difference Approximation method	Δx	Iriy*	Itire†	Time‡
Picard iteration method	First-order backward difference (BD), method	0·125	2	11	1·37
			3	17	5·32
		0·02	2	8	1·16
			3	11	3·92
		0·01	2	7	1·06
			3	14	4·54
	Second-order BD method	0·125	2	11	1·54
			3	18	6·13
		0·02	2	8	1·28
			3	14	5·11
		0·01	2	7	1·13
			3	13	4·81
Newton–Raphson method	First-order BD Method	0·125	2	10	1·45
			3	10	4·72
		0·02	2	7	1·36
			3	5	3·09
		0·01	2	6	1·07
			3	4	2·58
	Second-order BD method	0·125	2	10	1·79
			3	10	5·41
		0·02	2	7	1·44
			3	4	2·90
		0·01	2	6	1·20
			3	4	2·78
Newton–Raphson method	Crank–Nicolson method§	0·02	2	39	4·04
			3	39	14·73
		0·01	2	36	4·94
			3	36	14·38
		0·005	2	32	3·41
			3	32	12·20

*Interpolation rule, 2 for quadratic Lagrangian and 3 for cubic Hermite interpolation polynomial
†Required number of iterations
‡Does not include the pre-processor time
§The method diverged for $\Delta x = 0{\cdot}125$

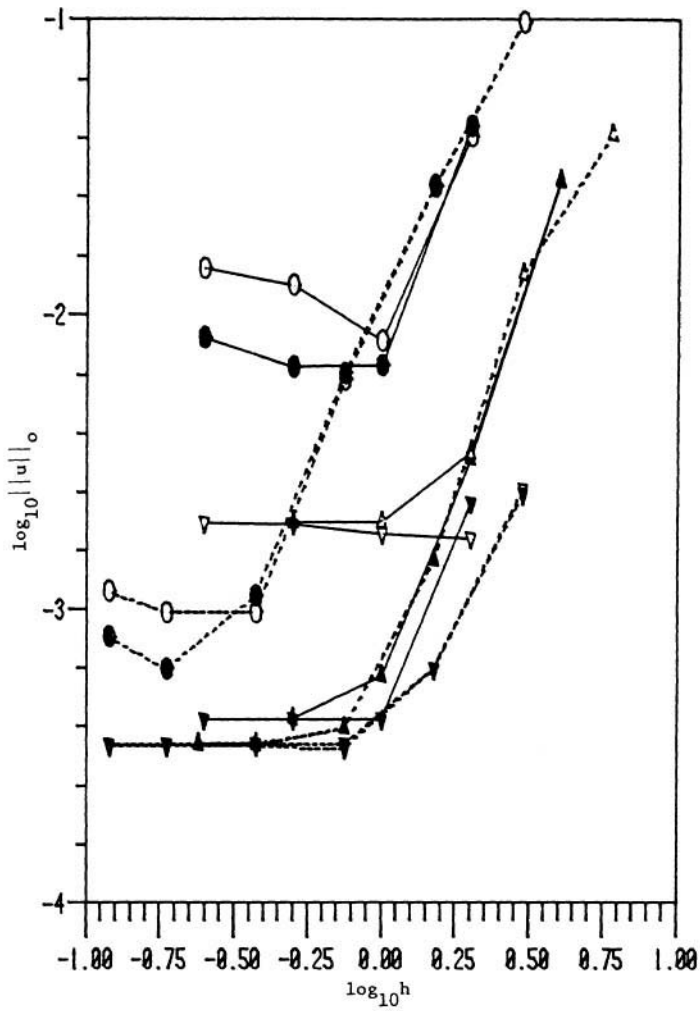

Figure 1. Convergence study; ———: $\Delta x = 0{\cdot}125$, – – –: $\Delta x = 0{\cdot}01$; ○; linear, △: Quadratic, ▽: Hermite element cases for one-step difference approximation; ●: linear, ▲: quadratic, ▼: Hermite element cases for two-step difference approximation

between the lower bounds become smaller as the grid size, Δx, becomes smaller. The quadratic Lagrangian and the first-order Hermite interpolation cases have nearly the same lower bound on convergence, whereas the bound for the linear element case is considerably larger than the other two interpolation cases. Figure 2 shows the effect of regrid upon convergence. It is found that the rate of convergence is not degraded by the regrid but the lower bound for convergence increases slightly after the regrid. Figures 1 and 2 also show that the convergence rates are quite different from those predicted by the finite element theory for linear parabolic problems. Another observation from Figures 1 and 2 is that the Hermite interpolation cases quickly approached the lower bound. Smooth, physically meaningful solutions were obtained beginning with only four elements in the space-like domain, as shown in Table II. Coarse grid inaccuracies, as was reported by Soliman and Baker,[9] were not observed in the present work. The required number of iterations for the Hermite interpolation case was about twice that of the Lagrangian interpola-

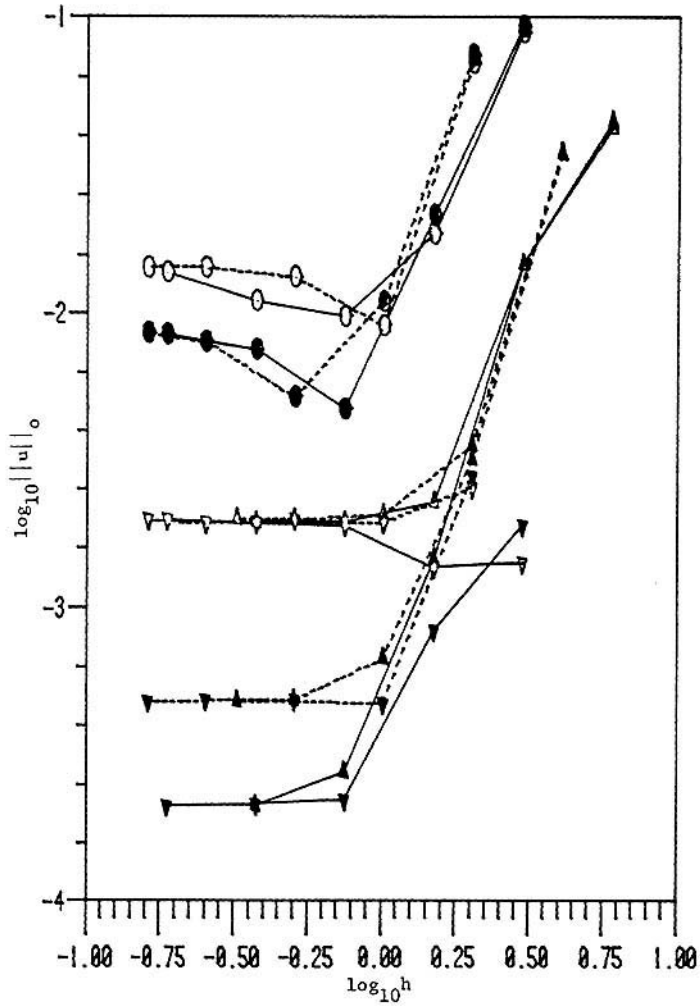

Figure 2. Effect of regrid on convergence; ———: no regrid, – – – –: regrid; Rest of the legends are the same as in Figure 1

tion case. The computer time required to generate each data point in Figures 1 and 2 ranged from two seconds, for the three Lagrangian element case, up to 25 seconds, for the one hundred Hermite elements with the first order difference approximation case. These computer times include data input, node generation, element generation, solution procedure, and the post-process. Computer time, to obtain a convergent solution for a data point, was less than four seconds for most of the cases. The number of iterations to achieve convergence for the first-order difference approximation method was about twice that of the second-order difference approximation method for all the cases.

Retarded Howarth flow

A boundary layer flow with a linearly retarded inviscid flow, which can occur on the aft portion of a certain aerofoil, was first studied by Howarth[17] using a series expansion method.

Table II. Coarse grid solutions for the flow over a flat plate

y	Data 1*	Data 2†		Blasius	
	u	u	$\partial u/\partial y$	u	$\partial u/\partial y$
0·0	0·0000	0·0000	0·2932	0·0000	0·2970
1·5	0·4372	—	—	0·4381	—
3·0	0·7879	0·7885	0·1778	0·7891	0·1763
4·5	0·9563	—	—	0·9570	—
6·0	0·9966	0·9958	0·0069	0·9958	0·0075
7·5	0·9997	—	—	0·9997	—
9·0	0·9999	0·9999	0·0000	0·9999	0·0000
10·5	0·9999	—	—	0·9999	—
12·0	0·9999	0·9999	0·	0·9999	0·0000
δ	1·928	1·926		1·925	
θ	0·7487	0·7428		0·7435	
c_f	0·3204	0·2943		0·2970	
$\|u\|_0$	0·0147	0·001817		—	
Itire	12	20		—	
Time	0·41 s	0·86 s		—	

*Four quadratic Lagrangian elements case
†Four cubic Hermite elements case
Data 1 and Data 2 are solutions at $x = 1{\cdot}25$ obtained by using the second order difference approximation.
Computer time does not include pre-processor routine such as data input and element data generation.

The inviscid tangential velocity outside of the boundary layer, on the physical domain, is given as

$$Ue(x) = b_0(1 - x/l), \tag{21}$$

where b_0 is the uniform upstream velocity and l is the length of the flat plate.

Consider a flat plate of length 1 m with a linearly retarded inviscid flow, the uniform upstream velocity of which is 35 m/s. Taking the reference length L to be 0·125 m and the reference velocity U_∞ to be 35 m/s yields the computational Reynolds number of $2{\cdot}995 \times 10^5$. Non-dimensionalizing equation (21) yields

$$\hat{U}e = 1 - \hat{x}/8, \tag{22}$$

where $\hat{U}e = Ue(x)/U_\infty$ and $\hat{x} = x/L$ are the non-dimensional velocity and tangential co-ordinates, respectively. For notational convenience, the superscript ($\hat{}$) is omitted in the following. The initial velocity data were obtained using Howarth's series expansion solution.[17] Since the boundary layer thickness grows rapidly in the flow direction, the computational domain in the normal direction was expanded and regrided in the solution procedure. To cope with the retarded inviscid flow and to locate the separation point more precisely, a variable grid size was used in the flow direction. The plot of convergence history for the retarded Howarth flow was almost the same as the flow over a flat plate case.[11] Among the six numerical schemes tested with several different grid sizes,[11] Lagrangian interpolation with second order difference approximation case yielded the most accurate and efficient results. Wall shear stresses evaluated by using 17 quadratic Lagrangian elements and second-order backward difference approximation with variable grid size in the flow direction; $\Delta x = 0{\cdot}02$ for $x < 0{\cdot}9$ and $\Delta x = 0{\cdot}001$ for $x < 0{\cdot}957$, are compared with those obtained by other investigators. The solution obtained by using 25 quadratic Lagrangian

Table III. Wall shear stress for the retarded howarth flow

x	Howarth	Bismark–Nasr[3]	Smith and Clutter[4]	Lynn and Alari[7]	Present analysis	
					Data 1*	Data 2†
0·10	2·739	2·7295	—	—	—	—
0·20	1·772	1·7714	1·7713	1·7354	1·7935	1·7713
0·30	1·309	1·3108	—	1·2337	1·3149	1·3130
0·40	1·011	1·0129	1·0106	0·9296	1·0077	1·0148
0·50	0·790	0·7911	—	0·7269	0·7812	0·7944
0·60	0·613	0·6101	—	0·5544	0·5987	0·6155
0·70	0·459	0·4544	—	0·3034	0·4405	0·4608
0·80	0·315	0·3072	0·316	0·2636	0·2909	0·3176
0·90	0·163	0·1470	—	0·1148	0·1216	0·1649
0·92	—	0·1075	0·128	0·0786	0·0740	0·1286
0·94	—	0·0723	—	0·960	—	0·0854
x_{sep}	0·96	0·950	0·960	0·9577	0·940	0.961

Wall shear stress represent $\sqrt{v(\partial u/\partial y)}/b_0^{1.5}$ where $\partial u/\partial y$ is evaluated on the physical co-ordinate
*First-order difference approximation case
†Second-order difference approximation case

elements with first-order difference approximation is also shown in Table III. The latter case overestimated the tangential velocity near the wall, hence larger wall shear stress, and underestimated the same velocity at the outer edge of the boundary layer, which caused early separation.

Flow over a circular cylinder

In the flow over a circular cylinder, the boundary layer separation causes a broad wake at the rear of the cylinder so that the inviscid velocity distribution is quite different from that of potential theory. The inviscid velocity distribution according to potential theory is given as[1]

$$Ue(\theta) = 2U_\infty \sin\theta, \tag{23}$$

whereas the same distribution due to the experiment by Hiemenz[1] is given as

$$Ue(\theta) = 2U_\infty(1{\cdot}814\theta - 0{\cdot}2710\theta^3 - 0{\cdot}0471\theta^5), \tag{24}$$

where θ is the angle measured in radians from the forward stagnation point. In the experiment, Hiemenz tried to keep the flow laminar as far as possible toward the rear of the cylinder. The radius Reynolds number was 9500 and the separation point was observed at about 80·5° from the forward stagnation point.

Both theoretical and experimental cases of the inviscid velocity distributions were considered in the present work.

Consider a circular cylinder of radius 0·27 m submerged in a uniform flow of 0·53 m/s, so that the resulting radius Reynolds number would be approximately 9800. Taking the reference length scale to be 1 m and the reference velocity to be the uniform upstream velocity yields the computational reference Reynolds number to be $3{\cdot}64 \times 10^4$. The initial velocity data at 5° from the forward stagnation point were obtained using the two-dimensional boundary layer flow near a stagnation point. The computed wall shear stresses are compared with other solutions in Table IV, where 25 quadratic Lagrangian elements and a second-order backward difference approximation with variable grid size in the flow direction was used for both of the cases.

Table IV. Wall shear stresses for the flow over a circular cylinder

	Experimental Ue		Analytical Ue	
θ deg	Data 1*	Smith and Clutter[4]	Data 2†	Terril[1]
10	1·2278	1·23	1·2273	1·23
20	1·2119	1·21	1·2106	1·21
30	1·1828	1·19	1·1827	1·19
40	1·1240	1·14	1·1419	1·14
50	1·0539	1·06	1·0860	1·06
60	0·9196	0·92	1·0155	1·02
70	0·6740	0·68	0·9129	0·91
75	0·4574	—	—	—
79	0·1394	—	—	—
79·3	0·0927	—	—	—
79·5	0·0479	—	—	—
80	—	—	0·7808	0·78
90	—	—	0·5958	0·59
100	—	—	0·3028	—
102	—	—	0·2121	—
103	—	—	0·1558	—
104	—	—	0·0788	—
104·2	—	—	0·0563	—
104·35	—	—	0·0334	—
θ_{sep}	79·65	80	104·55	104·5

Wall shear stresses represent $\partial u/\partial y \sqrt{(vx)}/Ue^{1\cdot5}$ where all the variables are evaluated on the physical co-ordinates

*$\Delta\theta = 1$ for $\theta < 65$, 0·2 for $\theta < 77$, and 0·05 for $\theta < \theta_{sep}$

†$\Delta\theta = 1$ for $\theta < 60$, 0·2 for $\theta < 100$, and 0·05 for $\theta < \theta_{sep}$

Table V. Wall shear stresses for the flow over a cone

x—FEM	Data 1*	Data 2†	F.S.‡
0·22	1·2016	1·2007	1·2002
0·30	1·0530	1·0525	1·0520
0·38	0·9523	0·9518	0·9514
0·46	0·8778	0·8775	0·8772
0·50	0·8472	0·8469	0·8467

The wall stresses represents $\partial u/\partial y$ on the FEM-computational co-ordinates

*25 quadratic Lagrangian elements with second-order difference approximation. $\Delta x = 0{\cdot}02$, Regrid at $x = 0{\cdot}16$ and 0·30

†25 quadratic Lagrangian elements with first-order difference approximation $\Delta x = 0{\cdot}01$, Regrid at $x = 0{\cdot}15$ and 0·28

‡Falkner–Skan similarity solution

Flow over a cone

Consider a boundary layer flow over a cone with half angle equal to 19·10° and axis aligned parallel to the undisturbed upstream flow direction. The inviscid velocity distribution of the surface of the cone is given as[1]

$$Ue(x) = U_1(x/L)^n, \tag{25}$$

where U_1 is a constant, x is the distance measured from the forward stagnation point along the surface of the cone, and $n = 0{\cdot}05$ when the half cone angle is 19·10°. The relationship between the cone angle and the exponent n is given in Reference 1.

Let $U_1 = 15$ m/s, x vary from 0·1 m to 0·5 m, and the reference length L be 1 m. Setting the reference velocity, U_∞, to be 15 m/s yields the computational Reynolds number of $1{\cdot}03 \times 10^6$ and the non-dimensionalized inviscid velocity as

$$\hat{U}e(\hat{x}) = \hat{x}^{0{\cdot}05} \tag{26}$$

The initial velocity data were obtained from the Falkner–Skan similarity solution.

The wall shear stresses are compared with the Falkner–Skan similarity solution at five locations in the flow direction in Table V.

SUMMARY AND CONCLUSIONS

A numerical procedure for boundary layer flows was developed using the semi-discrete Galerkin finite element method. The versatility and the convergence nature of the method were verified by computational experiments.

Convergence study showed that the Picard iteration technique was as good as the Newton–Raphson method for the Lagrangian interpolation case. It seems that the best solution technique depends on the physical problem to be solved and the other numerical factors used in the procedure. The convergence study also showed that the lower bound on convergence was determined not only by the discretization error in the time-like co-ordinate but also by the interpolation scheme used in the space-like domain. Also the convergence rates for each interpolation scheme were not comparable to those predicted by the linear theory. This convergence nature, different from the linear theory, is considered to be due to the feedback effect of the discretization error in the time-like co-ordinate into the semi-discretization procedure of the space-like domain through the normal velocity calculation. The lower bounds were almost the same for the quadratic Lagrangian and the first-order Hermite interpolation cases, but the lower bound was considerably larger for the linear Lagrangian element case. Therefore, the linear element was not suitable for boundary layer equations under the present formulation.

Coarse grid inaccuracies were not observed in the present study. The Hermite interpolation case yielded the most accurate solution for coarse grids. But, since the Hermite interpolation case required more iterations than the quadratic Lagrangian case for the same number of degrees of freedom, and hence longer computational time, and both have almost the same lower bounds, the quadratic Lagrangian element was found to be more practical for applications.

In general, the backward difference approximation is not suitable to study vibration of a class of dynamic systems since it introduces numerical viscosity and hence tends to yield optimistic results. This undesirable effect was not observed in the present study. The first-order difference approximation case overestimated the wall shear stresses and underestimated the tangential velocity near the outer edge of the boundary layer. Hence it predicted early separation.

On the other hand, the second order difference approximation case yielded a smaller lower

bound for the same grid size in the time-like co-ordinate. It also required fewer iterations than the first order difference approximation case. Among the several schemes tested, the quadratic Lagrangian element with the second-order backward difference approximation case was found to be more suitable for boundary layer equations than other schemes.

The regrid scheme, to cope with non-uniformly growing boundary layer thickness and to achieve computational efficiency, did not damage the convergence rate, but it slightly degraded the lower bound.

The computational results obtained by the present method compared favourably with solutions obtained by others. Considering the accuracy, efficiency, and the versatility, the method deserves to be extended to a wider class of boundary layer flows such as transient, compressible and turbulent cases.

REFERENCES

1. F. M. White, *Viscous Fluid Flow*, McGraw-Hill, New York, 1974.
2. H. Schlichting, *Boundary Layer Theory*, 3rd edn, McGraw-Hill, New York, 1974.
3. N. H. Bismark-Nasr, 'A finite difference-Galerkin finite element solution of compressible laminar boundary layer flows', *Int. J. Num. Meth. Eng.*, **12,** 711–719 (1978).
4. A. M. O. Smith and D. W. Clutter, 'Solution of the incompressible laminar boundary layer equation', *AIAA Journal*, 2062–2071 (1963).
5. T. Cebeci and P. Bradshaw, *Momentum Transfer in Boundary Layer*, McGraw-Hill, New York, 1977.
6. M. M. Gibson and W. Rodi, 'A Reynolds-stress closure model of turbulence applied to the calculation of a highly curved mixing layer', *J. Fluid. Mech.*, **103,** 161–182 (1981).
7. P. P. Lynn and K. Alani, 'Efficient least squares finite elements for two-dimensional laminar boundary layer analysis', *Int. J. Num. Meth. Eng.*, **10,** 809–825 (1976).
8. A. J. Baker, 'Laminar and turbulent boundary layer flow', in *Recent Advances in Numerical Methods in Fluids 1*, Pineridge, Swansea, U. K., 1980, pp. 287–309.
9. M. O. Soliman and A. J. Baker, 'Accuracy and convergence of a finite element algorithm for laminar boundary layer flow', *Computers and Fluids*, **9,** 43–62 (1981).
10. M. O. Soliman and A. J. Baker, 'Accuracy and convergence of a finite element algorithm for turbulent boundary layer flow', *J. Comp. Mtd. Applied Mechanics and Engineering*, **18,** 81–102 (1981).
11. S. W. Kim, 'Finite element method for incompressible laminar boundary layer flows', *Ph. D. Thesis*, A. E. Dept., University of Texas at Arlington, Arlington, Texas, 1983.
12. S. W. Kim and F. R. Payne, 'Finite element analysis of incompressible laminar boundary layer flows', *Proceeding of The Fifth International Symposium on Finite Elements and Flow Problems*, Austin, Texas, January 1984, pp. 231–236.
13. O. C. Zienkiewicz, *The Finite Element Method*, 3rd edn, McGraw-Hill, New York, 1977.
14. G. Strang and G. J. Fix, *An Analysis of the Finite Element Method*, Prentice-Hall, New Jersey, 1973.
15. J. T. Oden and J. N. Reddy, *An Introduction to the Mathematical Theory of Finite Elements*, Wiley, New York, 1976.
16. Z. Zlatev and P. G. Thomsen, 'Application of backward difference method to the finite element solution of time-dependent problems', *Int. J. Num. Meth. Eng.*, **14,** 1551–1061 (1979).
17. L. Howarth, 'On the solution of the laminar boundary layer equations', *Proc. Roy. Soc.*, **A164,** 547–588 (1938).